Supporting Information

for

Iridium(I)–Corrorin Complexes as Green-Light Photosensitizers for Singlet Oxygen

Yue Wang, [a] Yifan Wu, [a] Longxiang Wang, [a] Linxue Sang, [a] Jianfang Cao, [b] Hiroyuki Furuta, [c] Songlin Xue [a] and Ru Feng *[a]

[a] *School of Chemistry and Chemical Engineering, Jiangsu University, Zhenjiang 212013, China. E-mail: fengru@ujs.edu.cn*

[b] *School of Chemical Engineering, Ocean and Life Sciences, Dalian University of Technology, Panjin Campus, Panjin 124221, China*

[c] *Center for Supramolecular Chemistry and Catalysis, Department of Chemistry, College of Sciences, Shanghai University, Shanghai 200444, China*

Table of Contents

1. Instrumentation and Materials

All the chemicals were purchased and used without further treatment. Deionized water (DW) was used throughout the study. ^{1}H NMR spectra were recorded by a Bruker AVANCE II 400 spectrometer (400 MHz) in deuterated chloroform ($CDCl_3$). High-resolution mass spectra (HRMS) were obtained in electrospray ionization (ESI) mode on a Thermo Fisher Scientific Q Exactive Focus spectrometer, respectively. Crystallographic data were collected using a Rigaku XtaLAB Synergy-R diffractometer with Mo Kα radiation at 293 K. The structure was solved using a direct method (SHELXT) and refined using a full-matrix least-squares technique (SHELXL). The absorption spectra were recorded on UV-1780 (Shimadzu, Japan) spectrophotometer. The cyclic and different pulse voltammetry were conducted in a solution of 0.1 M TBAP in dry CH_2Cl_2 (distilled from CaH under reduced pressure) with a scan rate of 100 mV s^{-1} in an N_2-filled cell. A glassy carbon electrode and a platinum wire were used as a working and a counter electrode, respectively. A saturated Calomel electrode (SCE) was used as reference electrodes. The density functional theory (DFT) and time-dependent DFT calculations were performed with the Gaussian 16 program package[1]. The charge density difference maps were obtained via the "hole-electron" analysis[2] using Multiwfn program[3]. The energy gaps between the first singlet and triplet states (ΔE_{ST}) and the spin–orbit coupling (SOC) constants were calculated via ORCA program[4]. All isosurface graphics were rendered by VMD software[5].

2. Singlet Oxygen Generation Study

In the $^1O_2$ study, 1,3-diphenylisobenzofuran (DPBF) was employed as a representative singlet oxygen scavenger. The 3 mL of samples were prepared with a absorbance at 532 nm of ca. 0.8 in CH_3CN, then 50 μL of DPBF acetonitrile solution (20 mM) was added. The mixed soultion was measured on a UV-vis spectrometer, the solution was irradiated under 532 nm green laser beam (10 mW cm^{-2}) by a time interval of 0, 10, 20, 30, 40, 50, 60, 70, 80, 90, and 100 s, and Rose Bengal (RB) was used as standard photosensitizer, the decrease of DPBF asborption at 410 nm was monitored. The singlet oxygen quantum yields were calculated using the following formula:

$$\Phi_\Delta = \Phi_{\Delta\,ref} \times \frac{S_{sample}}{S_{ref}} \times \frac{I_{ref}}{I_{sample}}$$

$$I = 1–10^{-A}$$

Φ_Δ = singlet oxygen quantum yield, S = slope of the linear regression of the plot of the photobleaching rates of DPBF, I = absorbance correction factor. A = absorbance of the sample at irradiation wavelength (532 nm).

3. Ultrafast fs-TA measurements

The ultrafast fs-TA measurements were conducted on a fs pump-probe system in association with an amplified laser system under ambient conditions, which consist of a modelocked Ti:sapphire

seed laser (Spectra Physics, Maitai) directed to a regenerative amplifier (Spitfire Pro, Spectra Physics) and a high power laser (Empower, Spectra Physics) used for pumping and amplifier. The amplified 800 nm output was divided into two parts, and the pump pulses with tunable wavelength were generated by the major part of the beam (~85%) after an optical parametric amplifier (TOPAS prime, Spectra Physics), while the white-light continuum (WLC) probe and reference pulses (420−780 nm) were generated by the rest part of the beam passed through an optical delay line, here, the probe beam traveled through the sample and the reference beam was sent directly to the reference spectrometer. A chopper which can modulate the pump pulses was employed to obtain fs-TA spectra with and without the pump pulses alternately, and an optics fiber coupled to a multichannel spectrometer with a CMOS sensor was used to record the pump-induced fluctuation in probe/reference beam intensity with adjusting the optical delay line (maximum ~3ns). The spectral profiles were further processed by the Surface Xplorer.

4. Synthesis of FPh-Ir and Py-Ir

FPh-Ir. The bis(1,5-cyclooctadiene)iridium(I) dichloride (7.8 mg, 11.6 μmol) was added to the CH_2Cl_2 solution of pentafluorophenyl-substituted corrorin derivative (6 mg, 4 μmol). The reaction mixture was stirred under N_2 at reflux for 3 hours. After removal of the sovlent, the residue was purified by silica gel column chromatography (CH_2Cl_2/hexane = 1/1), the first purple fraction was collected to give **FPh-Ir** as purple solid (4.2 mg, 67.3%). ^{1}H NMR (400 MHz, $CDCl_3$): 14.16 (s, 1H), 12.67 (br, 1H) 7.31 (s, 1H), 7.16 (1H), 7.00 (1H), 6.88-6.87 (m, 1H), 6.79-6.78 (d, *J* = 5.1 Hz, 1H), 6.48 (s, 2H), 6.45 (d, *J* = 5.9 Hz, 2H), 6.32 (s, 1H), 6.24 (s, 1H), 6.17 (s, 1H), 3.83 (s, 1H), 3.77 (s, 1H), 3.07-3.02 (m, 2H), 2.88-2.84 (m, 2H), 2.78 (s, 1H), 2.65 (s, 1H), 2.40-2.33 (m, 2H). ESI-HR-MS: 1583.1470 $[M+H]^+$. UV-vis-NIR (in CH_2Cl_2) λ[nm] (ε [M-1cm-1]) 353 (54000), 540 (58000).

Py-Ir. The bis(1,5-cyclooctadiene)iridium(I) dichloride (19.8 mg, 29.4 μmol) was added to the CH_2Cl_2 solution of 2,6-dichloropyridyl-substituted corrorin derivative (15 mg, 12 μmol). The reaction mixture was stirred under N_2 at reflux for 3 hours. After removal of the sovlent, the residue was purified by silica gel column chromatography (CH_2Cl_2/hexane = 1/1), the first purple fraction was collected to give **Py-Ir** as purple solid (10.4 mg, 55.5%). ^{1}H NMR (400 MHz, $CDCl_3$): 14.31 (s, 1H), 12.71 (br, 1H), 8.57 (d, *J* = 11.3 Hz, 2H), 7.21 (s, 1H), 7.01-7.00 (m, 2H), 6.87 (s, 1H), 6.78 (d, *J* = 5.0 Hz, 1H), 6.52-6.46 (m, 4H), 6.35-6.34 (m, 1H), 6.31 (dd, *J* = 4.0, 2.3 Hz, 1H), 6.22 (s, 1H), 4.09 (t, *J* = 6.8 Hz, 1H), 3.66-3.63 (m, 1H), 3.12-3.11(m, 1H), 3.04-3.03 (m, 1H), 2.91-2.87 (m, 2H), 2.63-2.59 (m, 1H), 2.55-2.51 (m, 1H), 2.39-2.37 (m, 2H), 2.26-2.22 (m, 2H). ESI-HR-MS: 1563.1161 $[M+H]^+$. UV-vis-NIR (in CH_2Cl_2) λ[nm] (ε [M-1cm-1]) 369 (54800), 532 (58500).

5. HR-MS spectra

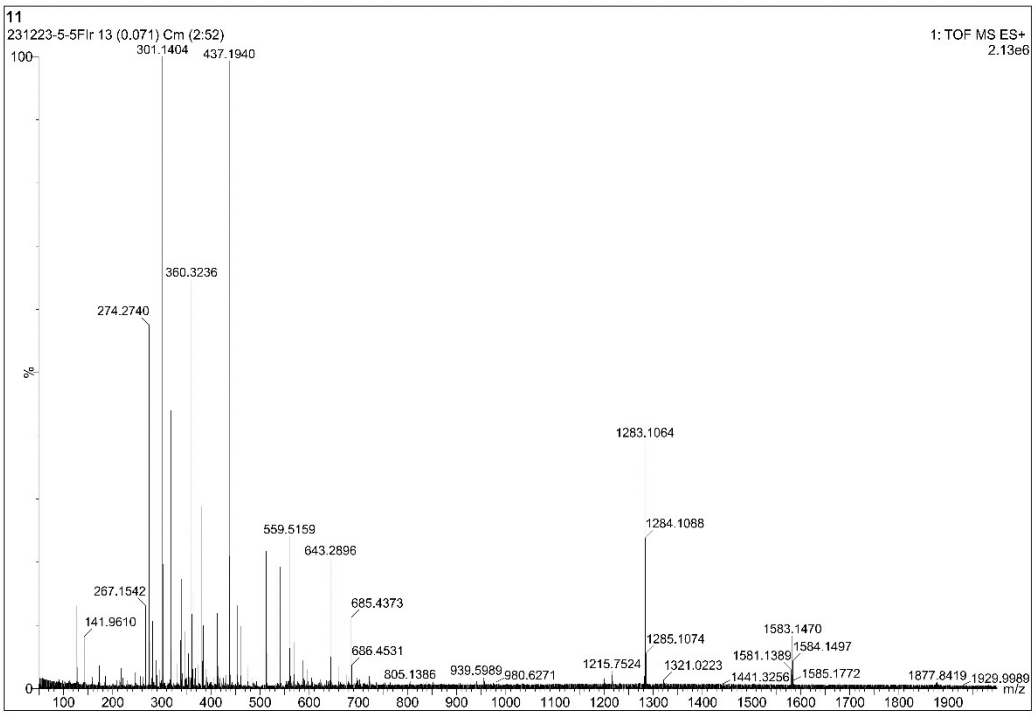

Figure S1. HR-ESI-TOF-MS spectrum of **FPh-Ir**.

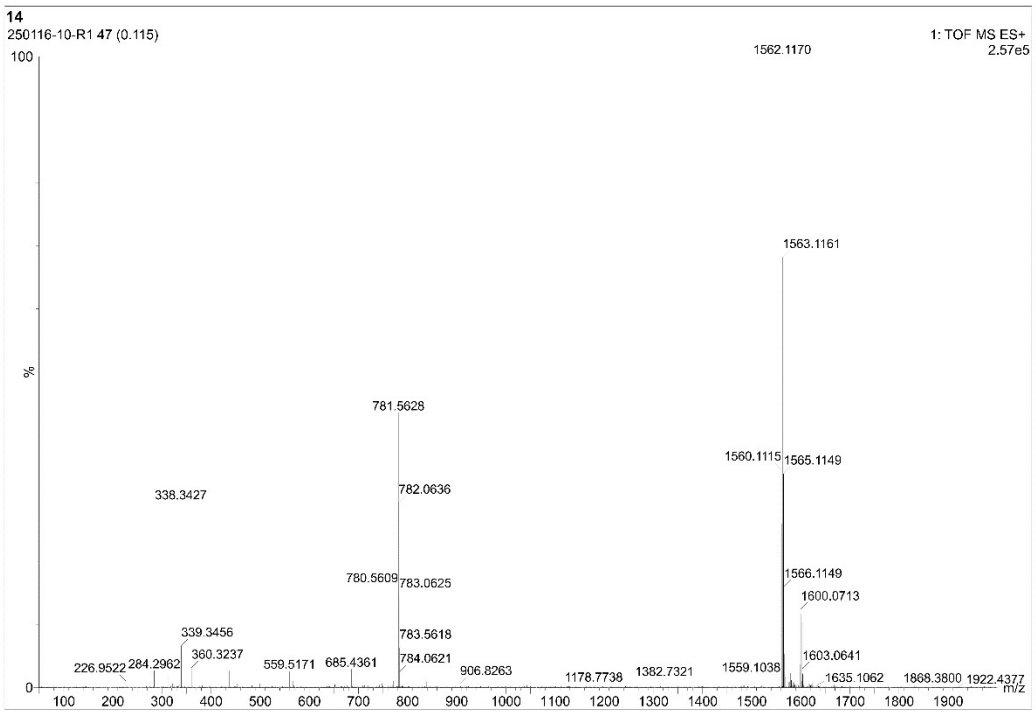

Figure S2. HR-ESI-TOF-MS spectrum of **Py-Ir**.

6. ^{1}H NMR spectra

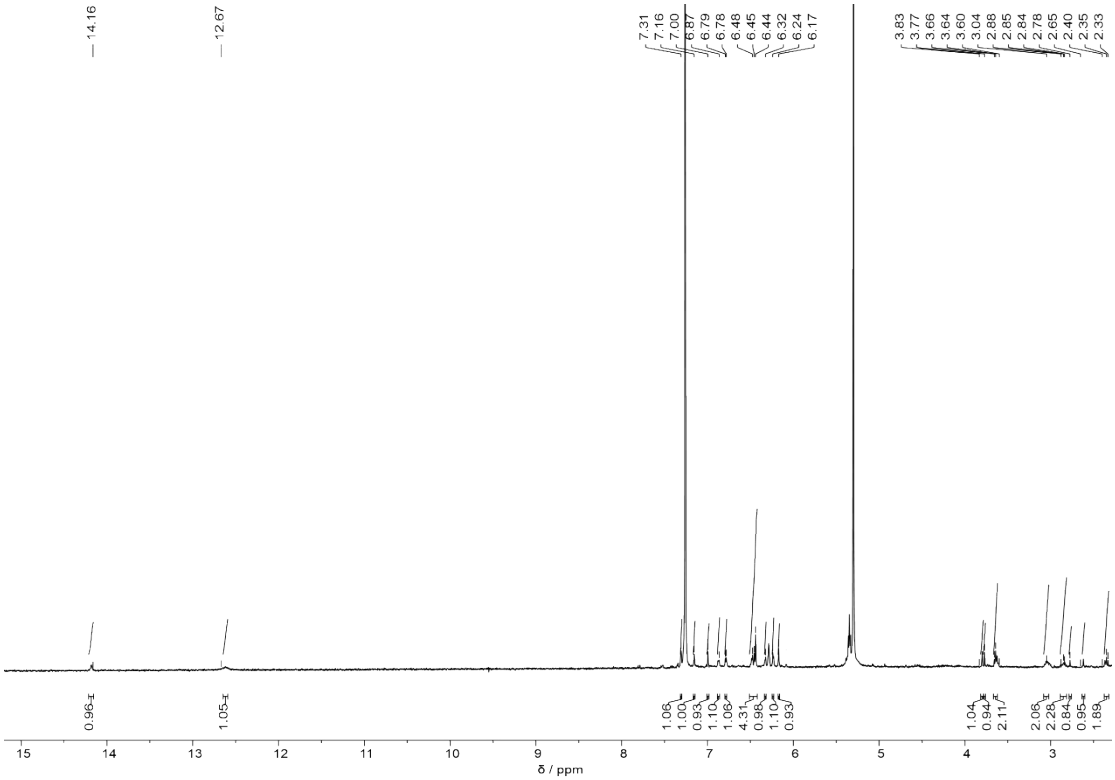

Figure S3. ^{1}H NMR spectrum of **FPh-Ir** recorded at 298 K in $CDCl_3$.

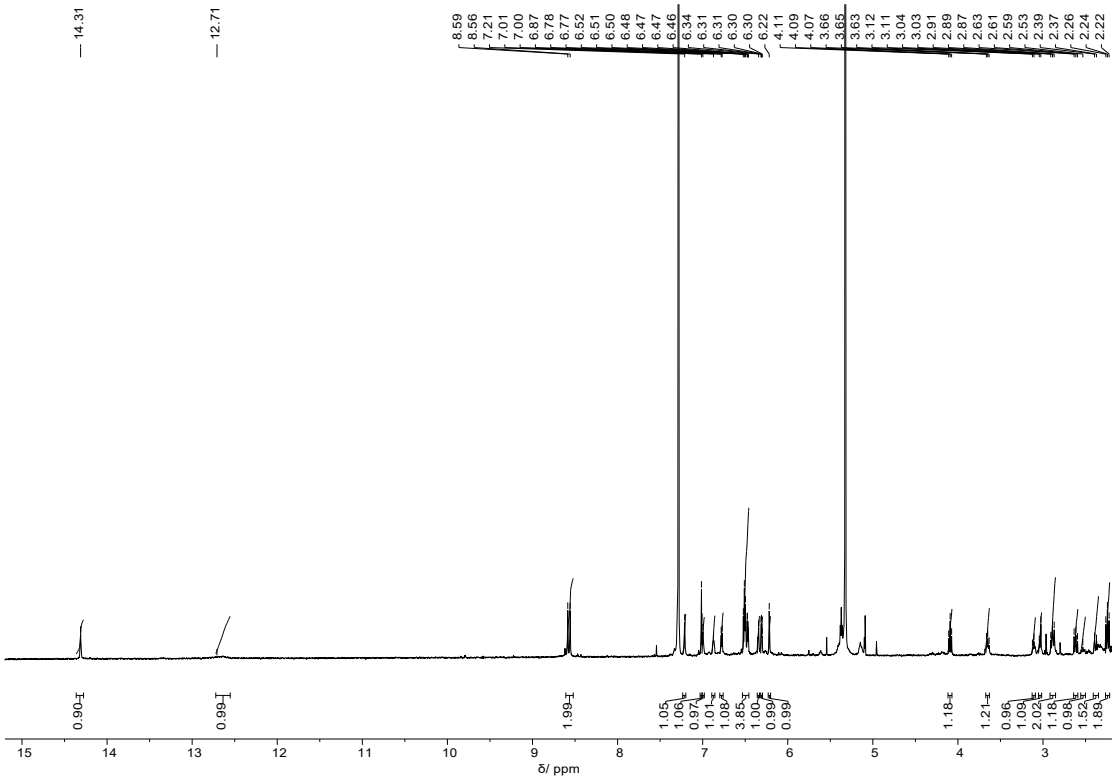

Figure S4. ^{1}H NMR spectrum of **Py-Ir** recorded at 298 K in $CDCl_3$.

7. Crystal data

Table S1. Crystallographic data for **Py-Ir**.

CCDC number	2499274
Empirical formula	$C_{66}H_{28}Cl_2F_{20}IrN_7$
Formula weight	1562.05
Temperature / K	193
Crystal system	monoclinic
Space group	$P2_1/n$
a / Å	17.1169(16)
b / Å	21.148(2)
c /Å	20.1177(19)
α / °	90
β / °	108.886(3)
γ / °	90
Volume / Å^3	6890.4(12)
Z	4
ρ_{calc}g/cm^3	1.506
μ/mm^{-1}	2.113
F_{000}	3056
Crystal size / mm^3	0.13 × 0.2 × 0.09
Radiation	MoKα (λ = 0.71073)
2θ range for data collection / °	3.792 to 50.7
Index ranges	$-20 \le h \le 20$, $-19 \le k \le 25$, $-24 \le l \le 22$
Reflections collected	50857
Independent reflections	12630 [R_{int} = 0.0940, R_{sigma} = 0.0910]
Data/restraints/parameters	127623/0/865
Goodness-of-fit on F^2	1.022
Final R indexes [I>=2σ (I)]	R_1 = 0.0559, wR_2 = 0.1079
Final R indexes [all data]	R_1 = 0.0970, wR_2 = 0.1249
Largest diff. peak/hole / e Å^{-3}	0.84/-0.83

8. UV-vis-NIR absorption spectra

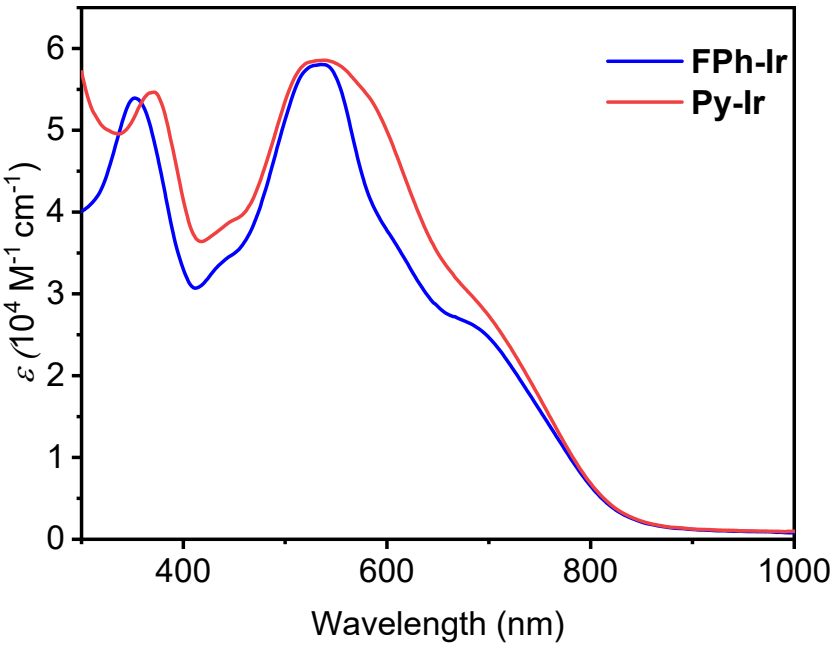

Figure S5. UV-vis-NIR absorption spectra of **FPh-Ir** (blue line) and **Py-Ir** (red line) in CH_2Cl_2 solution.

9. Theoretical calculation

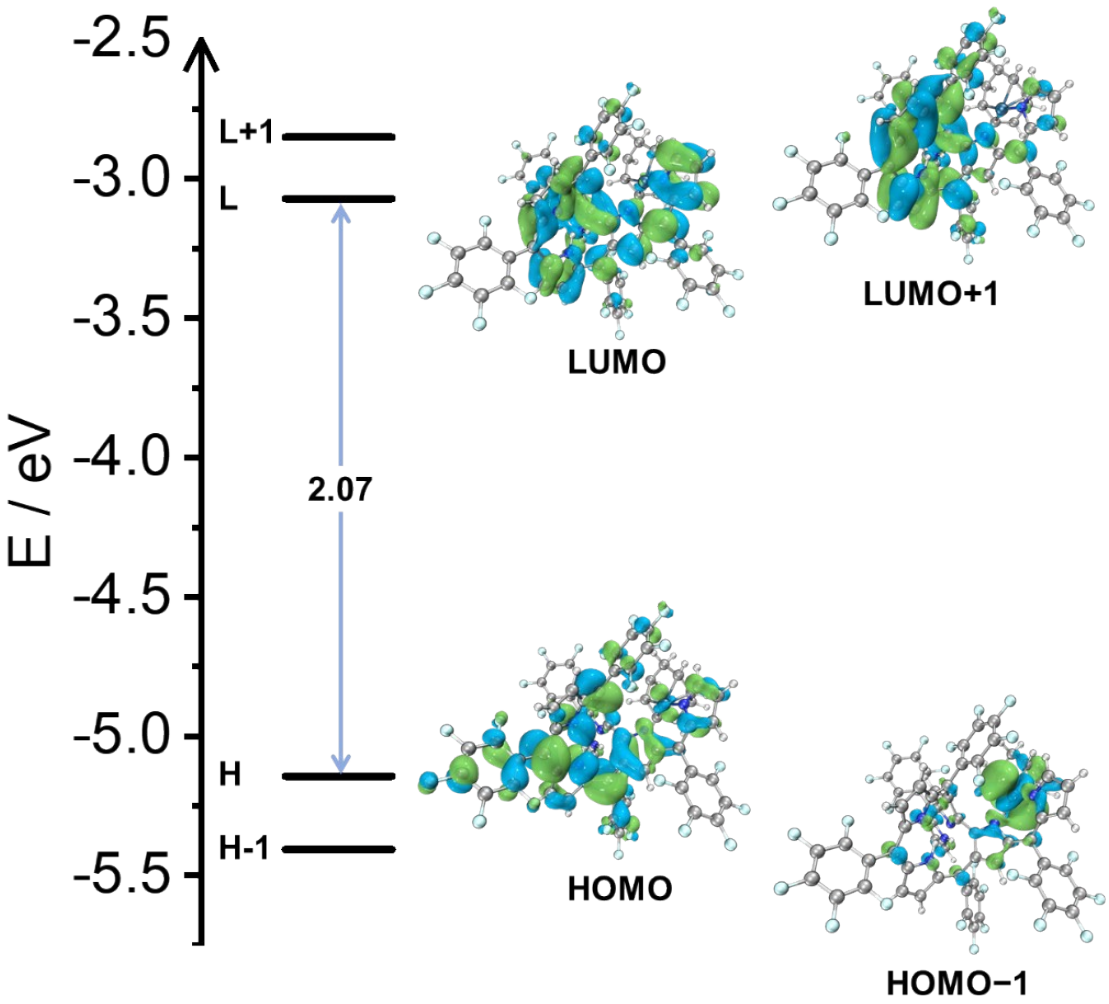

Figure S6. The molecular orbitals (isovalue = 0.02) and HOMO-LUMO gap of **PFPh-Ir**, calculated at the theoretical level of B3LYP/6-31G**+SDD.

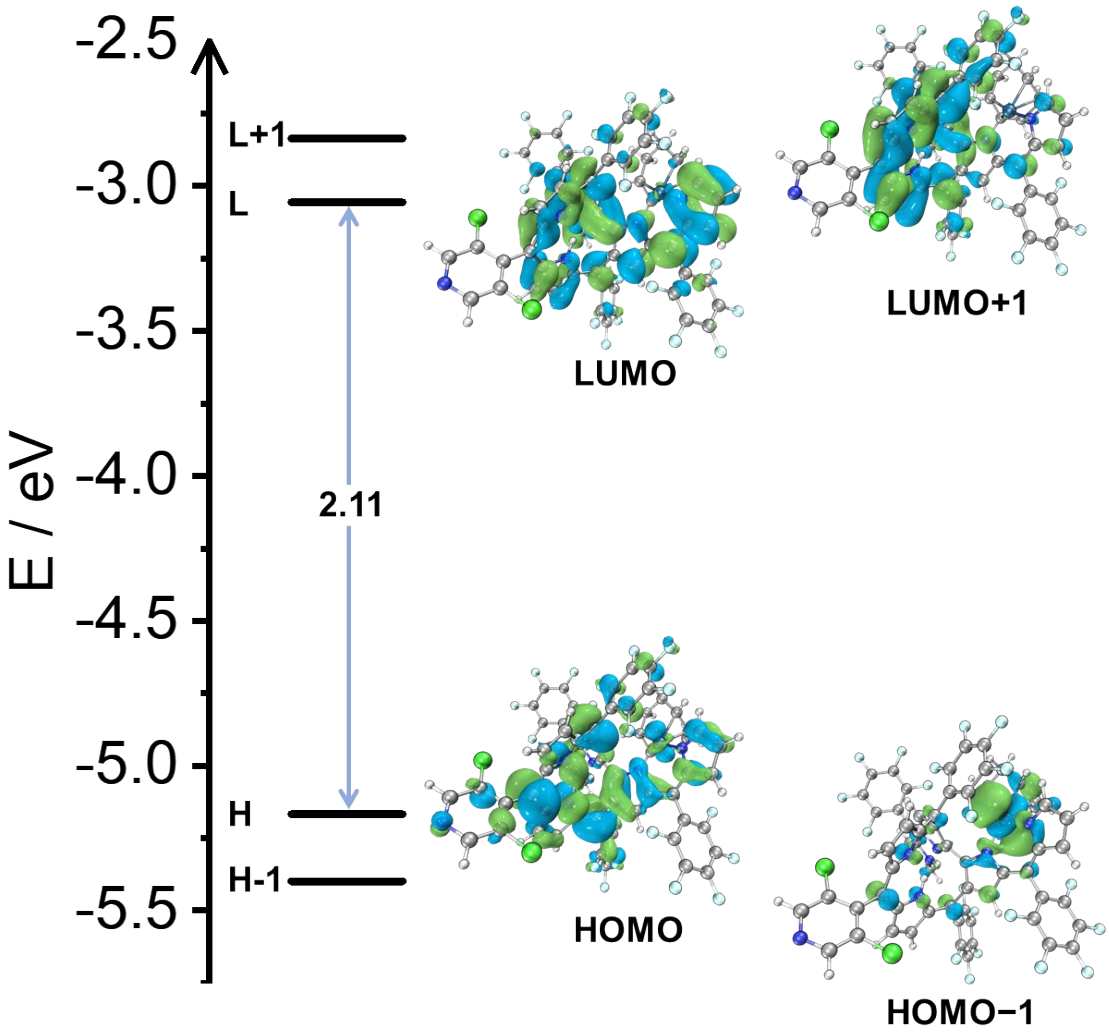

Figure S7. The molecular orbitals (isovalue = 0.02) and HOMO-LUMO gap of **Py-Ir**, calculated at the theoretical level of B3LYP/6-31G**+SDD.

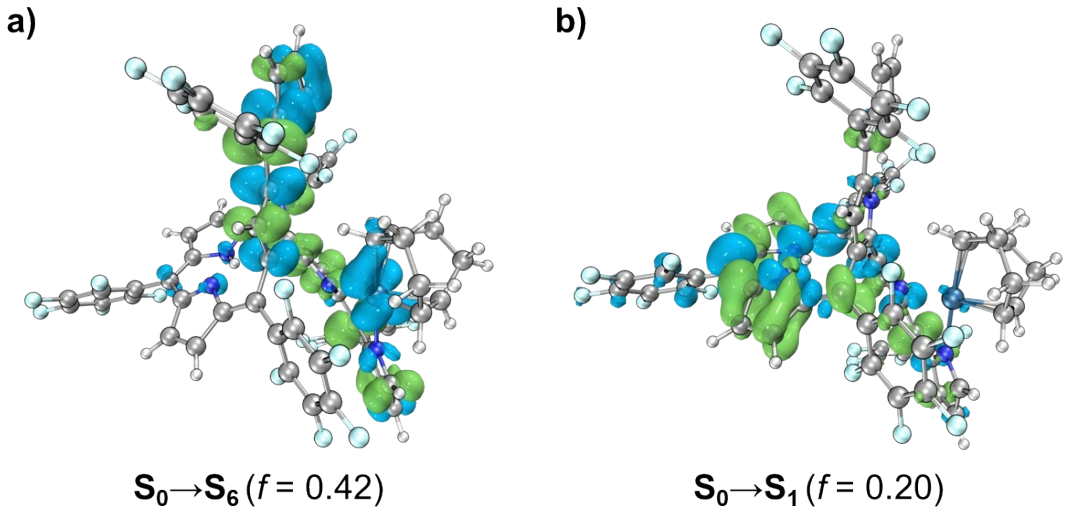

Figure S8. Charge density difference (CDD) maps of **FPh-Ir** in excitation states: **(a)** $S_0 \rightarrow S_6$ excitation and **(b)** $S_0 \rightarrow S_1$ (isovalue = 0.001). Green and blue regions denote the electron density depletion and accumulation, respectively. The CDD results were obtained from the TD-DFT calculation performed at theoretical level of CAM-B3LYP/6-31G**+SDD.

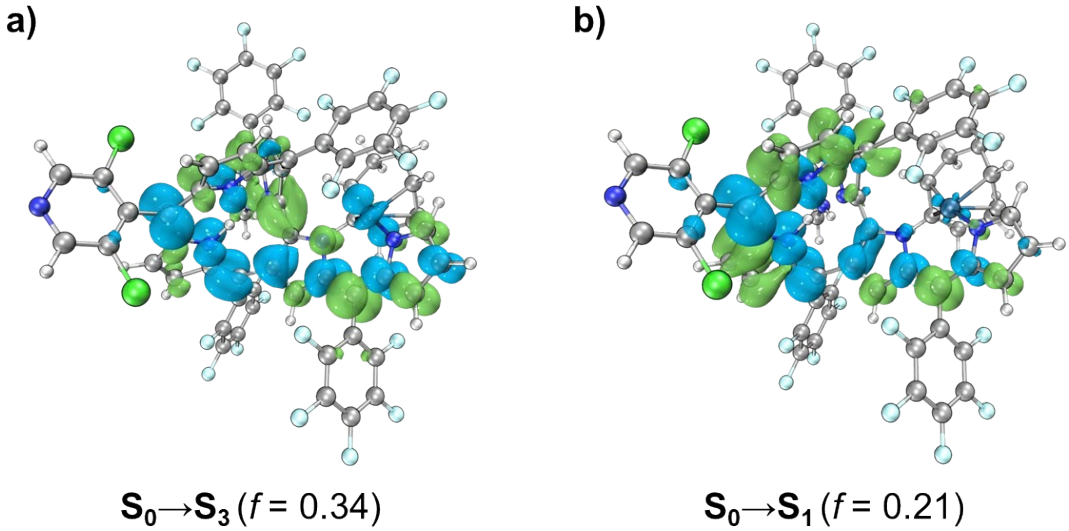

Figure S9. Charge density difference (CDD) maps of **Py-Ir** in excitation states: **(a)** $S_0 \rightarrow S_3$ excitation and **(b)** $S_0 \rightarrow S_1$ (isovalue = 0.001). Green and blue regions denote the electron density depletion and accumulation, respectively. The CDD results were obtained from the TD-DFT calculation performed at theoretical level of CAM-B3LYP/6-31G**+SDD.

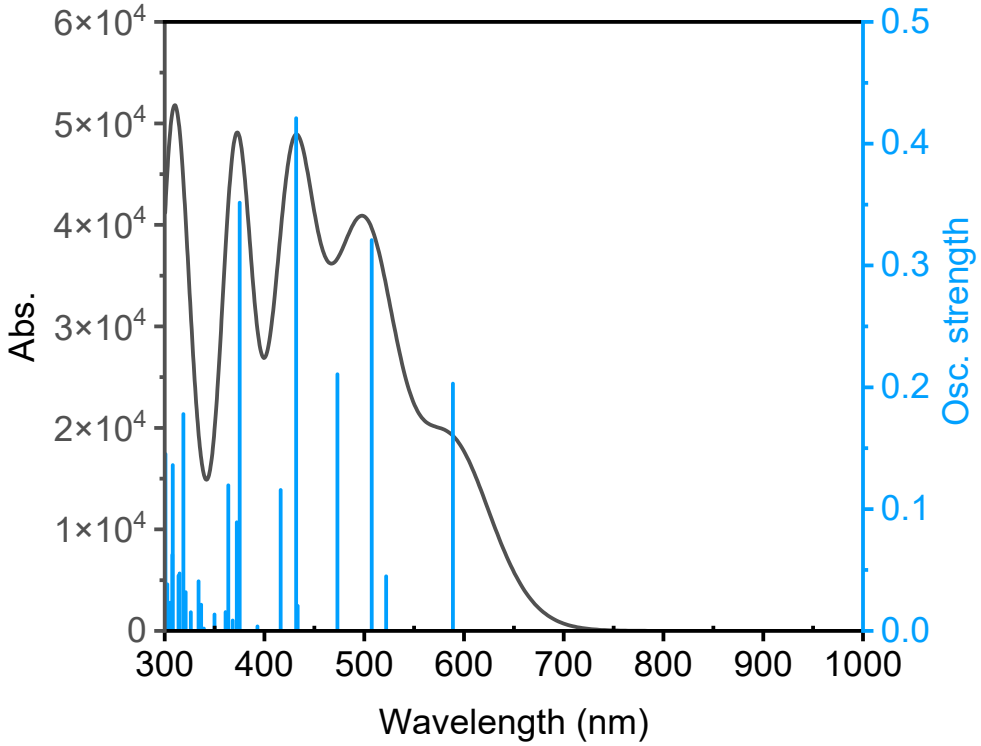

Figure S10. The simulated electronic absorption spectrum of **PF-Ir** with oscillators, calculated at the theoretical level of CAM-B3LYP/6-31G**+SDD.

Table S2. Selected TD-DFT (B3LYP/6-31G**+SDD) calculated energies, oscillator strength, and major molecular orbital contribution of **FPh-Ir**.

No.	Energy (cm-1)	Wavelength (nm)	Osc. Strength	Major contributions
1	16980.39	588.9146	0.203	HOMO->LUMO (65%), HOMO->L+1 (24%)
3	19703.32	507.5287	0.3209	H-2->LUMO (11%), HOMO->LUMO (12%), HOMO->L+1 (56%)
4	21134.15	473.1679	0.2107	H-1->LUMO (56%), HOMO->LUMO (14%)
6	23161.82	431.7449	0.421	H-3->LUMO (37%), H-1->LUMO (12%), HOMO->L+2 (17%)
7	24023.22	416.2639	0.1157	H-4->LUMO (39%), HOMO->L+2 (37%)
9	26657.43	375.1299	0.3516	H-5->LUMO (14%), HOMO->L+3 (47%)
12	27493.83	363.718	0.1196	H-3->L+1 (28%), HOMO->L+3 (26%)
20	31374.97	318.7254	0.178	H-6->LUMO (12%)
23	32462.2	308.0506	0.1361	H-6->LUMO (16%), H-3->L+2 (45%)
27	33242.95	300.8157	0.1452	H-5->L+1 (39%), H-1->L+3 (13%)

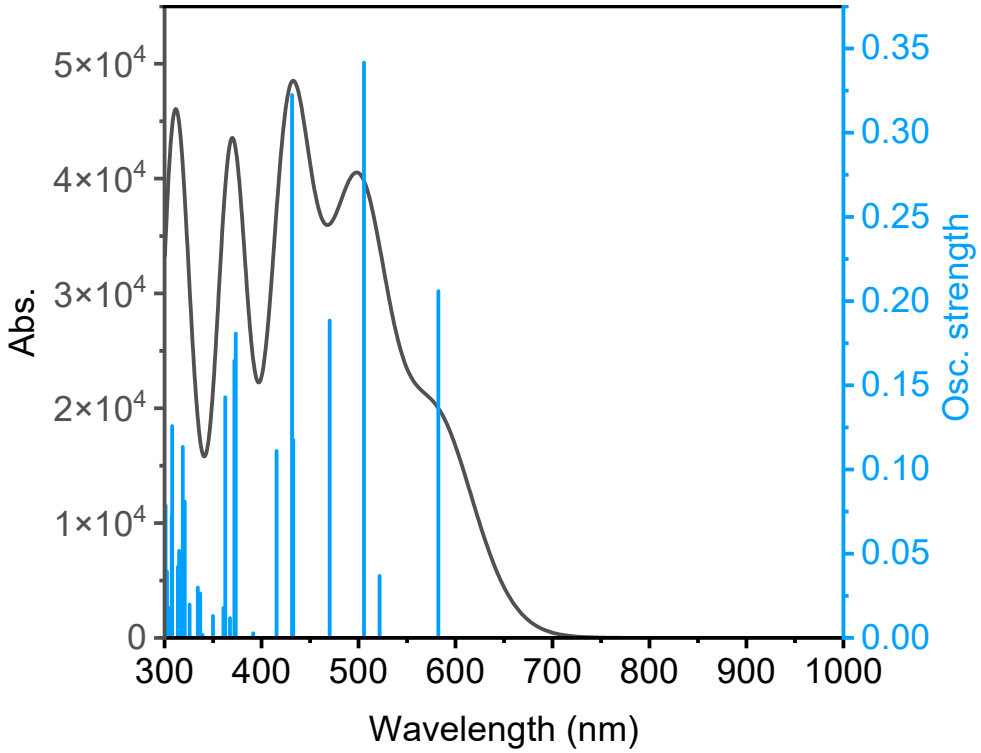

Figure S11. The simulated electronic absorption spectrum of **Py-Ir** with oscillators, calculated at the theoretical level of CAM-B3LYP/6-31G**+SDD.

Table S3. Selected TD-DFT (B3LYP/6-31G**+SDD) calculated energies, oscillator strength, and major molecular orbital contribution of **Py-Ir**.

No.	Energy (cm-1)	Wavelength (nm)	Osc. Strength	Major contributions
1	17172.35	582.3315	0.2059	HOMO->LUMO (66%), HOMO->L+1 (22%)
3	19775.1	505.6864	0.3417	HOMO->LUMO (12%), HOMO->L+1 (59%)
4	21262.39	470.3141	0.1884	H-1->LUMO (58%), HOMO->LUMO (12%)
5	23108.59	432.7395	0.1176	H-1->L+1 (76%)
6	23174.73	431.5045	0.3224	H-3->LUMO (32%), H-1->LUMO (21%), HOMO->L+2 (15%)
9	26784.87	373.3452	0.1807	H-5->LUMO (14%), H-3->L+1 (14%), H-2->L+1 (10%), HOMO->L+3 (28%)
10	26885.69	371.9451	0.1645	H-5->LUMO (10%), H-3->L+1 (10%), H-2->LUMO (10%), H-2->L+1 (40%)
12	27576.9	362.6223	0.1429	H-3->L+1 (22%), HOMO->L+3 (32%)
20	31371.74	318.7582	0.1134	H-6->LUMO (11%)
23	32479.95	307.8823	0.1258	H-6->LUMO (15%), H-3->L+2 (45%)

10. Electrochemical study

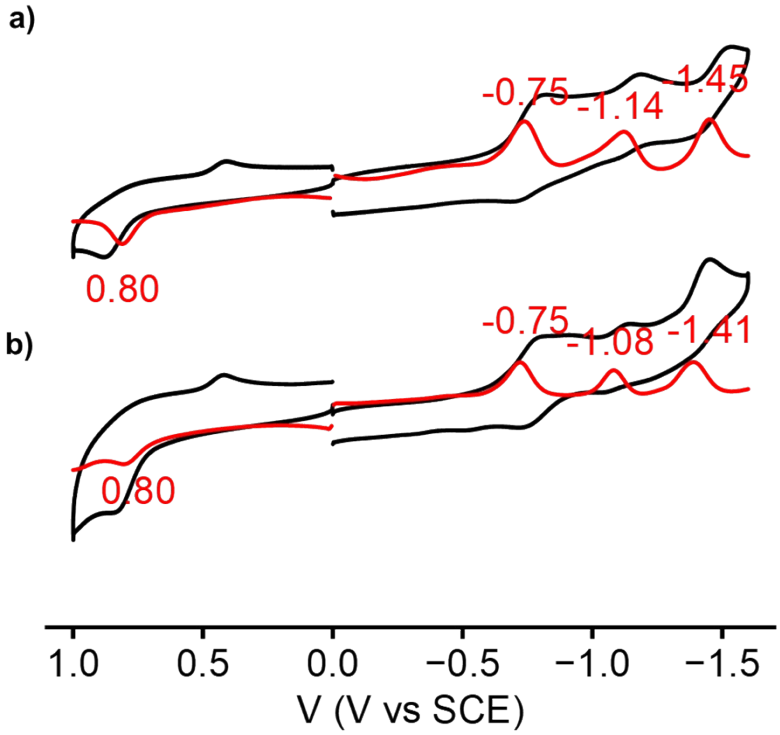

Figure S12. CVs (black lines) and DPVs (red lines) of **(a) FPh-Ir** and **(b) Py-Ir**.

11. Study of photostability

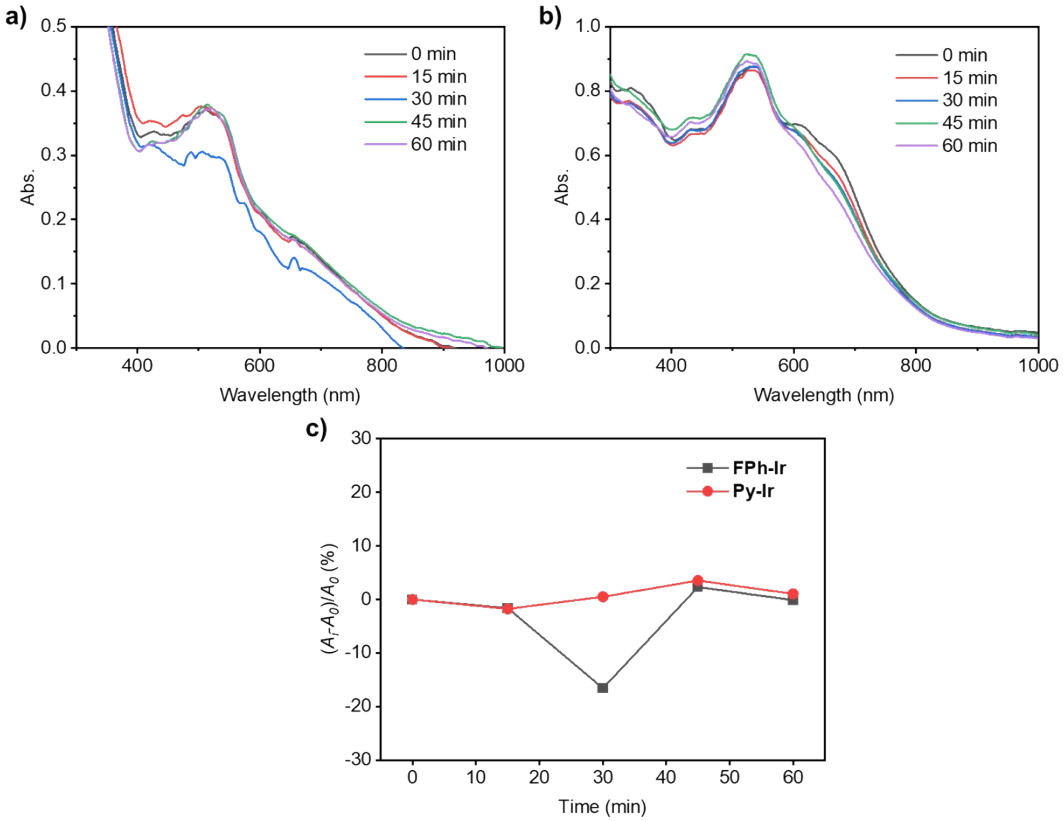

Figure S13. Time-dependent UV–vis absorption spectra of **(a) FPh-Ir** and **(b) Py-Ir** in CH_3CN under green-light irradiation with the optical density of 10 mW cm^{-2}, and **(c)** relative absorbance changes $(A_i - A_0) / A_0$ the characteristic absorption maxima (540 nm for **FPh-Ir** and 532 nm for **Py-Ir**) as a function of irradiation time. A_0 and A_i represent the absorbance before and after irradiation for a given time, respectively.

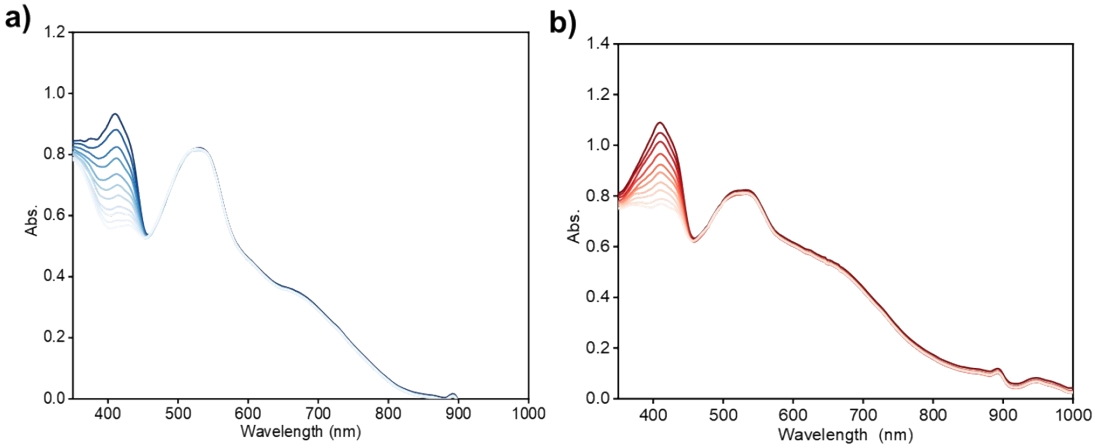

Figure S14. UV-vis absorption spectral changes of DPBF in the presence of **(a) FPh–Ir**, **(b) Py–Ir** with an expanded spectral region.

12. Study of spin-orbital constants (SOCs)

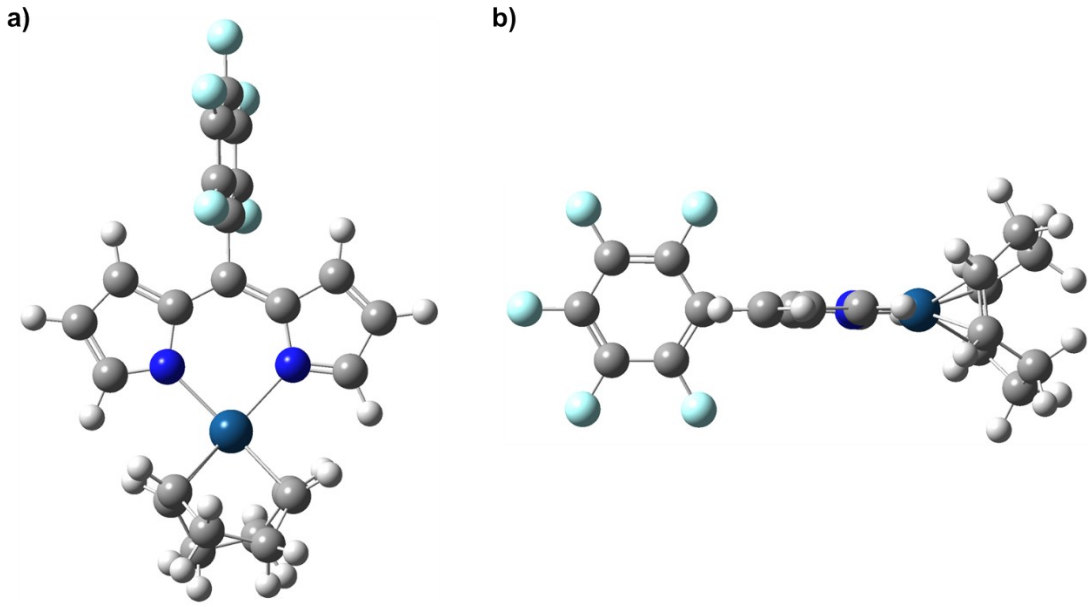

Figure S15. (a) Top view and **(b)** side view of optimized structure of **Dip-Ir**, obtained at the theoretical level of B3LYP/6-31G**+SDD.

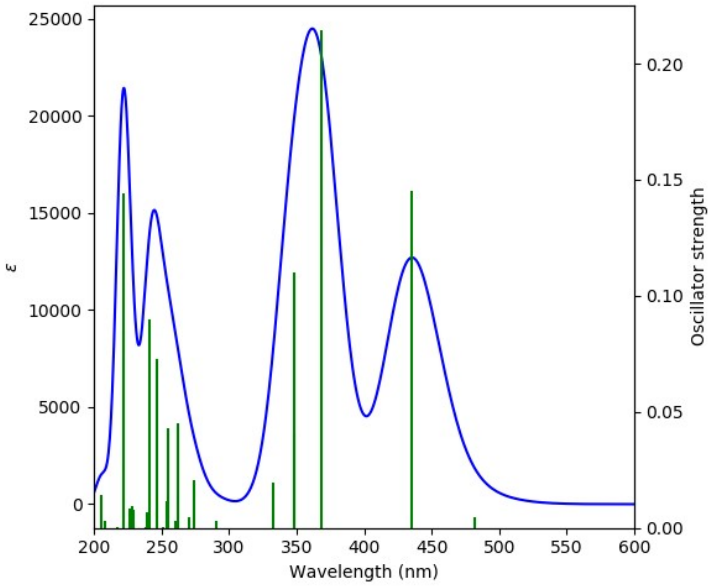

Figure S16. The simulated electronic absorption spectrum of **Dip-Ir** with oscillators, calculated at the theoretical level of CAM-B3LYP/6-31G**+SDD.

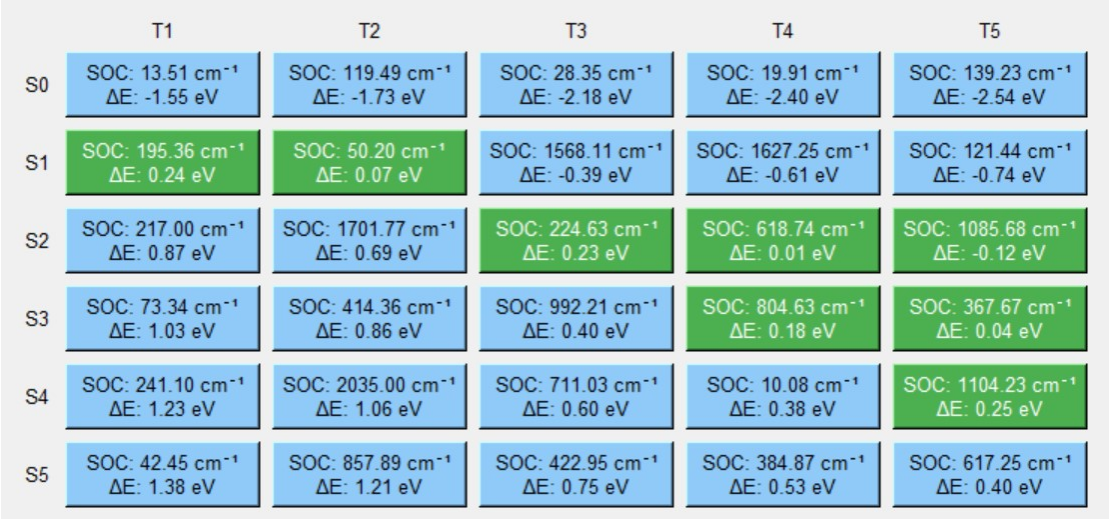

Figure S17. Calculated SOC constants of **Dip-Ir** between multiple singlet and triplet states, green blocks represent $|\Delta E_{ST}| < 0.3$ eV and SOC > 0.5 cm^{-1}, blue blocks represent fulfillment of either of the above conditions.

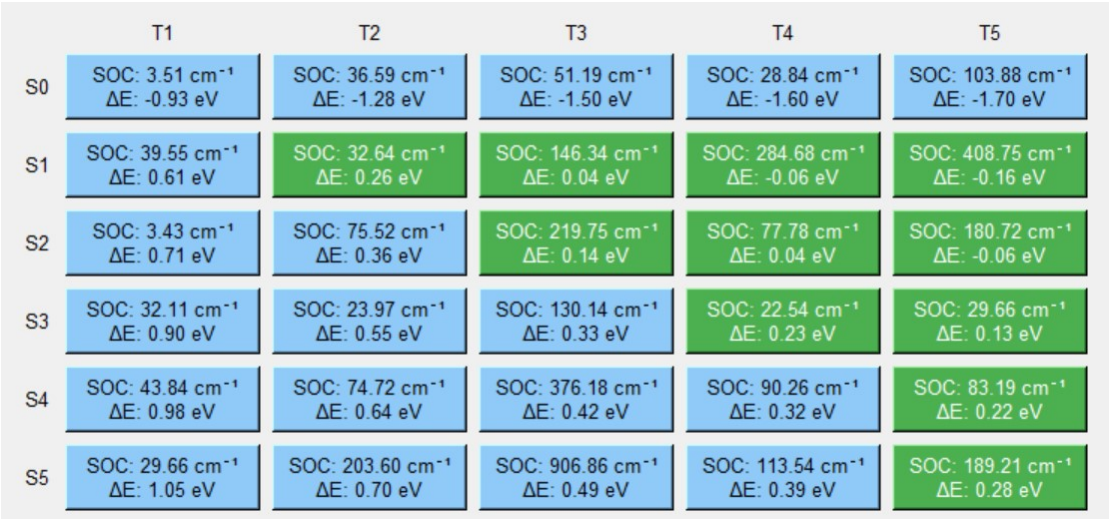

Figure S18. Calculated SOC constants of **PF-Ir** between multiple singlet and triplet states, green blocks represent $|\Delta E_{ST}| < 0.3$ eV and SOC > 0.5 cm^{-1}, blue blocks represent fulfillment of either of the above conditions.

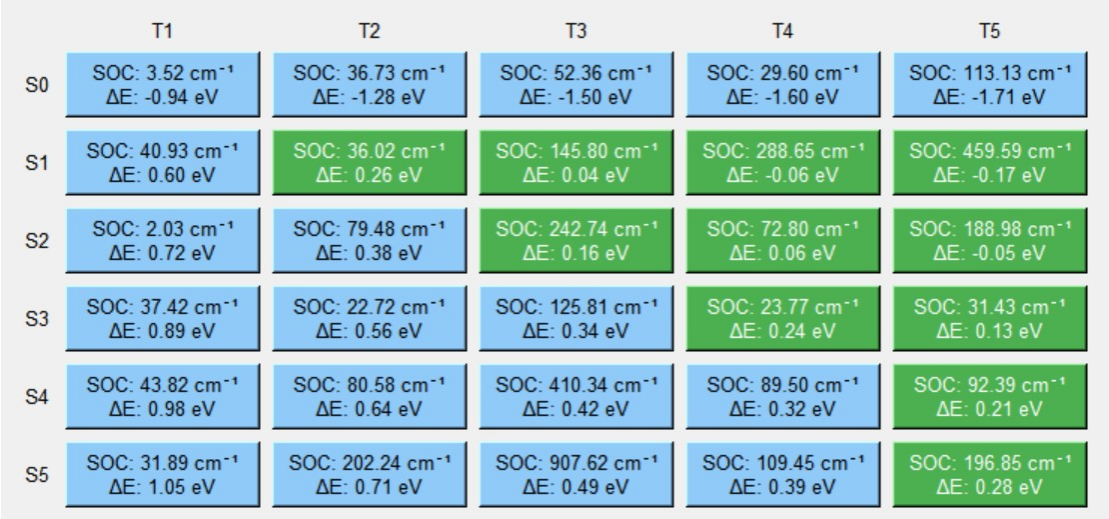

Figure S19. Calculated SOC constants of **Py-Ir** between multiple singlet and triplet states, green blocks represent $|\Delta E_{ST}| < 0.3$ eV and SOC > 0.5 cm^{-1}, blue blocks represent fulfillment of either of the above conditions.

Table S4. Cartesian coordinates of the DFT optimized geometry for **FPh-Ir**.

Energy = –5497.334463 hartree

Symbol	X	Y	Z	C	-0.13009	-5.6235	-0.64118
Ir	1.494999	-3.00816	-0.43372	H	-0.07513	-6.71995	-0.56338
F	6.166667	-1.69392	0.498631	H	-0.83327	-5.41717	-1.45324
F	8.455109	-0.29284	0.836127	C	-0.66921	-5.01194	0.669979
F	8.633727	2.272881	-0.07373	H	-1.7627	-4.98615	0.638258
F	6.506951	3.430852	-1.32831	H	-0.40862	-5.64556	1.524485
F	4.214162	2.038717	-1.67442	C	-0.15606	-3.59249	0.90461
F	2.510256	4.448963	2.836066	H	-0.92496	-2.83181	0.864242
F	3.499838	4.70187	5.311578	C	5.118189	0.130196	-0.59669
F	3.076803	2.758208	7.184648	C	6.22847	-0.4384	0.035175
F	1.624491	0.529455	6.518217	C	7.412104	0.272216	0.219686
F	0.65651	0.235435	4.047106	C	7.503893	1.583518	-0.24257
F	-6.12048	0.430738	2.705823	C	6.415118	2.175171	-0.87999
F	-8.54438	-0.54539	2.023647	C	5.239035	1.447466	-1.04927
F	-8.76791	-3.06374	0.998083	C	3.865117	-0.66331	-0.78675
F	-6.54189	-4.60553	0.665196	C	3.897863	-1.6535	-1.77227
F	-4.11452	-3.65082	1.353138	C	4.891323	-1.82958	-2.78777
F	-2.95324	-3.06479	-2.06813	H	5.781635	-1.22845	-2.90524
F	-2.27988	-5.14476	-3.60385	C	4.458845	-2.8565	-3.59943
F	-0.1873	-4.95846	-5.35536	H	4.934495	-3.24508	-4.48908
F	1.247285	-2.64324	-5.50769	C	3.232534	-3.31037	-3.04633
F	0.633599	-0.55943	-3.94649	H	2.614775	-4.1198	-3.40919
N	-0.4146	3.003304	0.173187	C	2.745334	-0.30086	-0.00858
H	-0.62534	2.12571	-0.32573	C	2.6619	0.799855	0.878488
N	-1.61138	1.754415	-1.62175	H	3.480282	1.443367	1.168797
N	-1.46173	-0.39878	1.69425	C	1.323814	0.988636	1.211295
N	-2.21337	-0.39988	4.283042	C	0.894879	2.175884	1.995894
H	-1.4486	-0.20686	3.63271	C	1.497769	2.349794	3.337994
N	1.472898	-0.85629	-0.16093	C	1.348058	1.358066	4.320459
N	2.886802	-2.60417	-1.96332	C	1.85625	1.484559	5.60714
C	1.004379	-3.28494	1.648707	C	2.582292	2.622047	5.952606
H	1.031981	-2.30706	2.128542	C	2.784604	3.616084	4.998718
C	1.950985	-4.29858	2.269131	C	2.253451	3.47071	3.718614
H	1.52214	-4.70497	3.197502	C	0.124443	3.163465	1.425128
H	2.861292	-3.76203	2.559067	C	-0.21503	4.532532	1.808704
C	2.32456	-5.43902	1.296348	H	0.065953	5.007907	2.736348
H	3.314401	-5.82835	1.555829	C	-0.86554	5.120459	0.765351
H	1.631639	-6.27982	1.402881	H	-1.21471	6.141536	0.717779
C	2.339409	-4.96054	-0.15561	C	-1.02446	4.129389	-0.29271
H	3.325608	-4.94951	-0.61812	C	-1.63771	4.155444	-1.55573
C	1.223605	-5.05614	-1.03155	C	-1.74926	2.903185	-2.27143
H	1.443425	-5.15739	-2.09453	C	-1.88088	2.637464	-3.71712

H	-2.03663	3.377848	-4.4907	C	-3.4923	-0.74183	6.079025
C	-1.72811	1.297384	-3.88232	H	-3.80936	-0.79847	7.110251
H	-1.76281	0.744759	-4.81131	C	-2.229	-0.34327	5.631499
C	-1.57905	0.725864	-2.53699	H	-1.34891	-0.04432	6.183393
C	-1.49005	-0.56117	-2.05987	C	-5.03537	-1.57318	2.047115
C	-1.20982	-1.70159	-2.95332	C	-6.19715	-0.81103	2.211529
C	-0.14542	-1.64644	-3.87205	C	-7.45333	-1.30065	1.861997
C	0.19578	-2.72341	-4.68299	C	-7.56905	-2.58538	1.335727
C	-0.52647	-3.91	-4.60002	C	-6.43096	-3.36997	1.162913
C	-1.58981	-4.00134	-3.70696	C	-5.18449	-2.86074	1.518798
C	-1.9161	-2.9135	-2.90548	C	-2.12318	5.410632	-2.15845
C	0.612913	-0.06595	0.520819	C	-3.39293	5.488706	-2.75634
C	-0.818	-0.36844	0.541534	C	-1.35362	6.585561	-2.19651
C	-1.70346	-0.73245	-0.58991	C	-3.87044	6.651988	-3.35208
C	-2.91108	-1.00767	-0.00489	C	-1.81747	7.764659	-2.77275
H	-3.82494	-1.26614	-0.51873	C	-3.08084	7.799324	-3.35754
C	-2.7591	-0.81843	1.418905	F	-4.20048	4.41703	-2.75536
C	-3.69294	-1.04328	2.423602	F	-5.08968	6.679544	-3.90288
C	-3.43675	-0.83995	3.811369	F	-3.53173	8.924131	-3.91927
C	-4.25059	-1.05601	4.943034	F	-1.04711	8.858937	-2.78638
H	-5.27101	-1.40995	4.92376	F	-0.11532	6.600192	-1.67756

Table S5. Cartesian coordinates of the DFT optimized geometry for **Py-Ir**.

Energy = –5936.419698 hartree

Symbol	X	Y	Z	F	3.369215	-5.04658	2.713314
Ir	-0.74112	-3.14285	-0.21631	F	1.253837	-5.72208	4.310347
Cl	3.49827	4.954184	3.407841	F	-0.68857	-3.87932	4.833541
Cl	-1.98337	5.552917	3.618972	F	-0.54637	-1.42118	3.787669
F	-5.55571	-2.72724	-1.22181	N	1.068731	7.503558	5.236341
F	-8.09802	-1.832	-1.44366	N	-0.23181	3.115373	0.576614
F	-8.89968	0.367503	-0.04286	H	0.164742	2.21712	0.897013
F	-7.14129	1.667939	1.586301	N	1.138709	1.786902	2.169634
F	-4.59695	0.780207	1.818833	N	1.585567	0.460634	-1.52299
F	-3.41436	4.41112	-1.87386	N	2.383675	1.223432	-3.98221
F	-4.41128	4.992884	-4.2916	H	1.578802	1.09274	-3.36562
F	-3.50245	3.697939	-6.51898	N	-1.21081	-1.03323	-0.0379
F	-1.55151	1.786911	-6.27285	N	-2.22729	-3.39797	1.254964
F	-0.56349	1.165052	-3.86997	C	-0.15334	-2.84716	-2.27042
F	5.961592	2.482787	-1.96605	H	-0.39859	-1.82015	-2.53956
F	8.524634	1.916371	-1.33088	C	-0.82373	-3.88772	-3.15146
F	9.283988	-0.66332	-0.87067	H	-0.29201	-3.97741	-4.11071
F	7.455288	-2.67951	-1.05723	H	-1.8277	-3.51844	-3.38865
F	4.893739	-2.13262	-1.70304	C	-0.94192	-5.26545	-2.46268
F	3.568518	-2.58545	1.693996	H	-1.80727	-5.80072	-2.86686

H	-0.06938	-5.88652	-2.68939	C	0.061173	4.211095	1.329681
C	-1.10072	-5.12749	-0.9484	C	0.615549	4.086525	2.61081
H	-2.07231	-5.43688	-0.56525	C	0.760794	5.260512	3.502091
C	-0.01343	-5.15817	-0.03291	C	-0.3326	6.00085	3.99901
H	-0.22782	-5.53192	0.968543	C	-0.13903	7.097256	4.842177
C	1.443558	-5.31112	-0.4332	H	-0.99754	7.651309	5.212295
H	1.647684	-6.34889	-0.73759	C	2.018531	5.722448	3.943881
H	2.060777	-5.13316	0.452057	C	2.128169	6.823015	4.79523
C	1.854848	-4.32655	-1.54922	H	3.109197	7.161368	5.117841
H	2.911144	-4.06519	-1.43415	C	1.003281	2.768617	3.053444
H	1.768775	-4.80269	-2.5318	C	1.174487	2.22992	4.416518
C	1.030366	-3.04091	-1.5246	H	1.150971	2.801679	5.335199
H	1.599586	-2.15485	-1.27488	C	1.329692	0.885842	4.28666
C	-4.99661	-0.99958	0.304354	H	1.479604	0.165197	5.079082
C	-5.92365	-1.64917	-0.51654	C	1.332907	0.603387	2.844205
C	-7.23501	-1.19737	-0.64387	C	1.557972	-0.53308	2.101954
C	-7.64511	-0.07274	0.069289	C	1.535191	-1.87487	2.715188
C	-6.74447	0.592899	0.898455	C	0.467324	-2.26237	3.545808
C	-5.43598	0.126482	1.006923	C	0.370499	-3.5391	4.088574
C	-3.59859	-1.51618	0.42576	C	1.353199	-4.48552	3.81444
C	-3.42699	-2.67804	1.183228	C	2.427669	-4.13834	3.001075
C	-4.38008	-3.28588	2.061484	C	2.50688	-2.8569	2.468145
H	-5.38934	-2.938	2.229384	C	-0.53906	0.057852	-0.47006
C	-3.74238	-4.34092	2.678542	C	0.922757	0.088456	-0.44299
H	-4.13896	-5.00809	3.431091	C	1.838894	-0.32141	0.648279
C	-2.42861	-4.38001	2.141551	C	3.091746	-0.1891	0.110107
H	-1.64916	-5.09052	2.378659	H	4.027326	-0.3522	0.623949
C	-2.57264	-0.75374	-0.17177	C	2.936911	0.280779	-1.24681
C	-2.72223	0.505159	-0.80251	C	3.922503	0.498927	-2.20229
H	-3.65944	0.999316	-1.01598	C	3.662262	0.95717	-3.52707
C	-1.4559	1.055055	-0.98077	C	4.532468	1.187515	-4.61303
C	-1.29857	2.453692	-1.45795	H	5.605535	1.064626	-4.59426
C	-1.91117	2.790292	-2.76504	C	3.752193	1.587219	-5.70647
C	-1.50913	2.121659	-3.9319	H	4.100084	1.840014	-6.69754
C	-2.02007	2.419961	-5.18885	C	2.420663	1.592876	-5.27985
C	-3.00168	3.399885	-5.31837	H	1.51039	1.81742	-5.8178
C	-3.45328	4.066207	-4.18218	C	5.339855	0.196564	-1.84975
C	-2.9158	3.756314	-2.93427	C	6.30352	1.206263	-1.75272
C	-0.78525	3.432415	-0.6378	C	7.628275	0.928981	-1.42392
C	-0.79238	4.894731	-0.6787	C	8.017211	-0.38743	-1.18593
H	-1.17307	5.493411	-1.49247	C	7.081425	-1.41531	-1.27797
C	-0.32418	5.357851	0.51468	C	5.761885	-1.11587	-1.60776
H	-0.24293	6.390993	0.821908				

Reference

(1) Frisch, M. J.; Trucks, G. W.; Schlegel, H. B.; Scuseria, G. E.; Robb, M. A.; Cheeseman, J. R.; Scalmani, G.; Barone, V.; Petersson, G. A.; Nakatsuji, H.; Li, X.; Caricato, M.; Marenich, A. V.; Bloino, J.; Janesko, B. G.; Gomperts, R.; Mennucci, B.; Hratchian, H. P.; Ortiz, J. V.; Izmaylov, A. F.; Sonnenberg, J. L.; Williams-Young, D.; Ding, F.; Lipparini, F.; Egidi, F.; Goings, J.; Peng, B.; Petrone, A.; Henderson, T.; Ranasinghe, D.; Zakrzewski, V. G.; Gao, J.; Rega, N.; Zheng, G.; Liang, W.; Hada, M.; Ehara, M.; Toyota, K.; Fukuda, R.; Hasegawa, J.; Ishida, M.; Nakajima, T.; Honda, Y.; Kitao, O.; Nakai, H.; Vreven, T.; Throssell, K.; Montgomery Jr., J. A.; Peralta, J. E.; Ogliaro, F.; Bearpark, M. J.; Heyd, J. J.; Brothers, E. N.; Kudin, K. N.; Staroverov, V. N.; Keith, T. A.; Kobayashi, R.; Normand, J.; Raghavachari, K.; Rendell, A. P.; Burant, J. C.; Iyengar, S. S.; Tomasi, J.; Cossi, M.; Millam, J. M.; Klene, M.; Adamo, C.; Cammi, R.; Ochterski, J. W.; Martin, R. L.; Morokuma, K.; Farkas, O.; Foresman, J. B.; Fox, D. J. *Gaussian 16 Revision C.01*; Gaussian, Inc.: Wallingford CT, 2016.

(2) Liu, Z.; Lu, T.; Chen, Q. An Sp-Hybridized All-Carboatomic Ring, Cyclo[18]Carbon: Electronic Structure, Electronic Spectrum, and Optical Nonlinearity. *Carbon* **2020**, *165*, 461–467. https://doi.org/10.1016/j.carbon.2020.05.023.

(3) Lu, T.; Chen, F. Multiwfn: A Multifunctional Wavefunction Analyzer. *J. Comput. Chem.* **2012**, *33* (5), 580–592. https://doi.org/10.1002/jcc.22885.

(4) Neese, F. Software Update: The ORCA Program System—Version 6.0. *WIREs Comput. Mol. Sci.* **2025**, *15* (2), e70019. https://doi.org/10.1002/wcms.70019.

(5) Humphrey, W.; Dalke, A.; Schulten, K. VMD: Visual Molecular Dynamics. *J. Mol. Graph.* **1996**, *14* (1), 33–38. https://doi.org/10.1016/0263-7855(96)00018-5.